ISSN (e): 2250 – 3005 || Volume, 14 || Issue, 3|| May. - June. – 2024 ||
International Journal of Computational Engineering Research (IJCER)

Entropy Generation in Unsteady Oscillatory MHD Flow with Thermal Radiation and Binary Chemical Reaction

Sunday O. Olokor[1], Mathew O. Alabi[2] and Akindele M. Okedoye[3,]
[1]Research Student, Department of Mathematics, Federal University of Petroleum Resources, Effurun, Nigeria.
[2]Professor, Department of Physical Sciences, College of Natural and Applied Sciences, Chrisland University, Abeokuta, Nigeria.
[3]Professor, Department of Mathematics, Federal University of Petroleum Resources, Effurun, Nigeria.
[3]Corresponding Author: **okedoye.akindele@fupre.edu.ng**

ABSTRACT
This article considered a comprehensive Second Law analysis of unsteady oscillatory magnetohydrodynamic (MHD) flow past a moving plate, incorporating thermal radiation and binary chemical reaction dynamics. By integrating insights from fluid dynamics, MHD, heat transfer, and chemical reaction kinetics, the study offers a multidisciplinary exploration of complex fluid systems influenced by interacting phenomena. Through numerical simulations, concentration, temperature, and velocity profiles are scrutinized, providing critical insights into fluid behavior and heat transfer mechanisms under varying conditions. The impact of key parameters such as Hartmann number, porosity, radiation parameter, and chemical reaction parameter is thoroughly examined, highlighting their influence on system performance and efficiency. Utilizing the Bejan number for entropy generation analysis, the study emphasizes understanding thermodynamic limitations and irreversibilities within the system to guide optimization efforts. Sensitivity analysis reveals the intricate interplay between different parameters, aiding engineers in optimizing processes and system designs. This interdisciplinary endeavor contributes to a deeper understanding of fluid dynamics and heat transfer phenomena, with implications for aerospace, energy systems, and environmental science, paving the way for the development of more efficient and sustainable technologies and processes.

KEYWORDS: Entropy Generation in Unsteady Oscillatory MHD Flow with Thermal Radiation and Binary Chemical Reaction

AMS Subject Classification: 76D05, 76D07, 76N10, **35Q35**.

Date of Submission: 09-05-2024 Date of acceptance: 23-05-2024

I. INTRODUCTION

Several researchers have explored thermal hydromagnetic fluid flow with buoyancy-induced flows, rotating fluids, and chemical binary reactive fluid flow in the presence of activation energy. Early studies include [1] examination of transient viscous, incompressible, rotating fluid flow over an infinite permeable wall, and [2] investigation of oscillating flow of rotating fluid past a vast half-plate. Additional works by [3], [4] and [5] have further contributed to this field.

Thermally developed Falkner-Skan bioconvection flow of magnetized nanofluid with motile gyrotactic microorganisms, finding that radiation and magnetic parameters boost the Nusselt number was investigated by [6]. The heat storage units using Y-shaped fins for solidification of NEPCM was presented by [7], while Maleque [8] provided solutions for unsteady temperature and species transport of natural convective flow through permeable surfaces. Other studies, such as those by [9], [10] and [11], have examined various aspects of MHD flow, including radiative effects, porous media interactions, and chemical reactions, providing comprehensive insights into the complex dynamics of these systems.

The study of entropy generation in unsteady oscillatory magnetohydrodynamic (MHD) flow with thermal radiation and binary chemical reactions is crucial for understanding the thermodynamic behavior of complex fluid systems. MHD flows involve the interaction between magnetic fields and electrically conducting fluids, which introduces additional layers of complexity due to Lorentz forces that significantly influence fluid motion and heat transfer characteristics ([12]; [13]). When combined with unsteady oscillatory conditions, these flows exhibit intricate temporal variations that impact energy dissipation and entropy generation ([14]).

Thermal radiation, a critical mode of heat transfer in high-temperature environments, modifies the thermal energy distribution within the fluid and influences entropy production ([15]). Binary chemical reactions, involving two reacting chemical species, add another dimension of complexity by introducing mass transfer and associated chemical energy changes, affecting the overall irreversibility of the system ([16]). The coupled effects of thermal radiation and chemical reactions in an oscillatory MHD flow necessitate a comprehensive analysis to quantify entropy generation accurately ([17]).

Entropy generation, a measure of irreversibility, is influenced by various factors, including viscous dissipation, Joule heating due to electrical currents, heat conduction, and mass diffusion ([18], [19]). Understanding the contributions of these factors under the combined influence of oscillatory flow, magnetic fields, thermal radiation, and chemical reactions is essential for optimizing system performance and enhancing energy efficiency ([20]; [21]). This study aims to explore these interactions, providing insights into the fundamental thermodynamic processes governing entropy generation in such complex fluid systems, with implications for various engineering applications, including energy systems, industrial processes, and environmental management ([22], [5]).

The estimated impact of the free convection on oscillatory flow using data to predict the value of the attributes to promote concentration for mass transfer was presented by [23]. Results were obtained concerning the concentrations constructed and plotted graphically, taking into consideration three values of the time. We then focused on the statistical technique used to analyze the neural network problem of predicting the concentration of free convection oscillatory flow. In the work of [24], the effects of magnetic field and porosity on entropy generation and Bejan number in sodium-alginate (C6H9NaO7) fluid over a moving, heated vertical wall with free convection are studied through analytical solutions and numerical computations, revealing significant impacts on velocity, entropy generation, and Bejan number, with increased Hartmann number enhancing entropy generation and more porous media reducing entropy generation by up to 50%.

Due to its essential usefulness in engineering systems, entropy generation of reactive hydromagnetic flows are often follow with heat transfer as encountered in several systems of engineering. Many machines operate under diff er harsh conditions with various types of fluids as lubricants. Largely, the lubricating oils viscosity often reduces as the temperature increases. This variation in the viscosity of lubricant will definitely aff ect its efficiency. Fluid flow in motion dissipates kinetic energy, transforming it into internal energy, leading to fluid heating. Despite existing research on diverse flow types, a knowledge gap exists in determining entropy generation for the specific case of: Unsteady mixed convection (buoyancy and forced flow), Oscillatory flow behavior (e.g., sinusoidal), Electrically conducting fluid, Moving plate boundary, Mass transfer (species diff usion), Thermal radiation, Binary chemical reaction (with activation energy). Hence this current research is aimed at studying entropy generation in unsteady oscillatory MHD flow with thermal radiation and binary chemical reaction.

II. Mathematical/Problem formulation

Consider an unsteady unidimensional convective flow of a viscous incompressible fluid with radiative heat transfer and chemical reaction past a flat plate moving through a binary mixture. Let the x-axis be taken along the plate in the direction of the flow and the y-axis be taken normal to it. A magnetic field of uniform strength B_0 is applied in the direction of flow and the temperature field is neglected. Initially, the plate and the fluid are at same temperature T_w in a stationary condition with concentration level C_w at all points. At time $t > 0$ the plate starts oscillating in its own plane with a velocity U_0. Its temperature is raised to Tw and the concentration level at the plate is raised to C_w. The ambient condition is given by φ_∞ (where $\varphi = \{u, T, C\}$) and the part associated with motion called, dynamic part φ_d is given as $\varphi_d = \varphi - \varphi_\infty$. The suffix ∞ in the derivatives is omitted since it is a constant. The binary chemical reaction follows the one used by [25], [26], [27]. The velocity component is in y -direction. The continuity equation could be written as

$$\frac{\partial v}{\partial y} = 0 \tag{2.1}$$

Under the Boussinesq's approximation, the fluid momentum, energy and species concentration equations in the neighborhood of the plate is described by the following respectively

$$\frac{\partial u}{\partial t} + v\frac{\partial u}{\partial y} = -\frac{1}{\rho}\frac{\partial p}{\partial x} + v\frac{\partial^2 u}{\partial y^2} + g\beta_T(T - T_\infty) + g\beta_C(C - C_\infty) - \frac{\sigma}{\rho}B_0^2 u \tag{2.2}$$

$$\rho C_p\left(\frac{\partial T}{\partial t} + v\frac{\partial T}{\partial y}\right) = k\frac{\partial^2 T}{\partial y^2} + Q(T - T_\infty) - \frac{\partial q_r}{\partial y} \tag{2.3}$$

$$\rho\left(\frac{\partial C}{\partial t} + v\frac{\partial C}{\partial y}\right) = D_f\frac{\partial^2 C}{\partial y^2} - R_A \tag{2.4}$$

where Q is the heat of chemical reaction.

Using the Roseland approximation for radiative heat transfer and the Roseland approximation for diffusion, the expression for the radiative heat flux q_r can be given as

$$q_r = \left(\frac{-4\bar{\sigma}}{3k_s}\right)\left(\frac{\partial T^4}{\partial y}\right) \tag{2.5}$$

Here in equation (2.5), the parameters $\bar{\sigma}$ and k_s represent the Stefan Boltzmann constant and the Roseland mean absorption coefficient, respectively.

Now on assuming that the temperature differences within the fluid flow are sufficiently small, T^4 in equation (2.5) can be expressed as a linear function of T_∞ ' using the Taylor series expansion. The Taylor series expansion of T^4about T_∞ , after neglecting the higher order terms, takes the form

$$T^4 \cong 4T_\infty^3 T - 3T_\infty^4 \tag{2.6}$$

We employed chemical reaction of Arrhenius type of the *1st* order irreversible reaction given by,

$$R_A = k_r^2(T - T_\infty)^n \exp\left(-\frac{E_a}{R_G T}\right)(C - C_\infty) \tag{2.7}$$

where k_r is the reactivity of chemical reaction defined by frequency of collision ω and orientation factor p as $k_r = k_r(\omega, p) = \omega p$, R_G is the universal gas constant.

The appropriate initial and boundary conditions relevant to the problem are

$$\left.\begin{array}{c} t = 0: u = U_0, v = v_w(t), T = T_w, C = C_w\ \forall y \\ t > 0: \begin{cases} u = U_1, T = T_w + A_1 e^{i\omega t}, C = C_w + A_2 e^{i\omega t}, y = 0 \\ u \to U(t), T \to T_\infty, C \to C_\infty\ as\ y \to \infty \end{cases} \end{array}\right\} \tag{2.8}$$

where U_0 is the plate characteristic velocity. $A_1, A_2 > 0$ and $A_1 = (T_w - T_\infty)$, $A_2 = (C_w - C_\infty)$.

At free stream, $u \to U, T \to T_\infty, C \to C_\infty$ while at time $y = 0$, the suction/blowing is a function of stream velocity given as

$$v(0,t) = -v_0 \cdot U(t) = -v_0(1 + \epsilon e^{i\omega t}) \tag{2.9}$$

with $v_0 > 0$ being the suction velocity and $v_0 < 0$, the blowing or injection velocity.

Following [25] and [26], the continuity equation (2.1) on integration becomes

$$v(y,t) = v_w(t)$$

At free stream, as $y \to \infty, u \to U, T \to T_\infty, C \to C_\infty$; and substituting this into equation (2.2) yields,

$$-\frac{1}{\rho}\frac{\partial p}{\partial x} = \frac{\partial U}{\partial t} + \frac{\sigma B_0^2}{\rho}U \tag{2.10}$$

then, using equation (2.10) in equation (2.2)-(2.4) gives

$$\frac{\partial u}{\partial t} + v\frac{\partial u}{\partial y} = \frac{\partial U}{\partial t} + v\frac{\partial^2 u}{\partial y^2} + g\beta_T(T - T_\infty) + g\beta_C(C - C_\infty) - \frac{\sigma B_0^2}{\rho}(u - U) \tag{2.11}$$

$$\rho C_p\left(\frac{\partial T}{\partial t} + v\frac{\partial T}{\partial y}\right) = k\frac{\partial^2 T}{\partial y^2} + Q(T - T_\infty) + \frac{16\bar{\sigma}T_\infty^3}{3k_s}\frac{\partial^2 T}{\partial y^2} \tag{2.12}$$

$$\rho\left(\frac{\partial C}{\partial t} + v\frac{\partial C}{\partial y}\right) = D_f\frac{\partial^2 C}{\partial y^2} - k_r^2(T - T_\infty)^n \exp\left(-\frac{E_a}{R_G T}\right)(C - C_\infty) \tag{2.13}$$

III. **Entropy Generation Rate** (Γn)

According to [18] the characteristics entropy transfer rate is given by

$$\Gamma_0 = k\left(\frac{\Delta T}{LT_0}\right)$$

Where k, L, T_0 and ΔT are respectively, the thermal conductivity, the characteristics length of the enclosure, a reference temperature and a reference temperature difference.[28, give two-dimensional entropy generation rate as

$$\begin{aligned}\Gamma = \mu/T_0\left[2\left(\frac{\partial u}{\partial x}\right)^2 + 2\left(\frac{\partial v}{\partial x}\right)^2 + \left(\frac{\partial v}{\partial x} + \frac{\partial u}{\partial y}\right)^2\right] + K/T_0^2\left[\left(\frac{\partial T}{\partial x}\right)^2 + \left(\frac{\partial T}{\partial y}\right)^2\right] \\ + \frac{RD}{C_0}\left[\left(\frac{\partial C}{\partial x}\right)^2 + \left(\frac{\partial C}{\partial y}\right)^2\right] + \frac{RD}{T_0}\left[\left(\frac{\partial T}{\partial x}\right)\left(\frac{\partial C}{\partial x}\right) + \left(\frac{\partial T}{\partial y}\right)\left(\frac{\partial C}{\partial y}\right)\right]\end{aligned} \tag{3.1}$$

Where C_0 and T_0 are respectively the reference concentration and temperature, which are in our case, the bulk concentration and the bulk temperature.

A. Non – Dimensionalisation

Defining conveniently the following dimensionless quantities;

$$\left.\begin{aligned} y = \frac{vy'}{v_0}, v' = \frac{v}{v_0}, u' = \frac{u}{U_0}, t' = \frac{tv_0^2}{4v}, U' = \frac{U}{U_0}, \omega' = \frac{4\omega v}{v_0^2}, V = \frac{U_1}{U_0} \\ \theta(y,t) = \left(\frac{E_a}{R_G T_\infty^2}\right)(T - T_\infty) = \frac{T - T_\infty}{\epsilon T_\infty}, \qquad \emptyset(y,t) = \frac{C - C_\infty}{C_w - C_\infty}\end{aligned}\right\} \tag{3.2}$$

Using the dimensionless quantities (3.2) in equations (2.11) – (2.13) and (3.1), we have after dropping the primes we have:

$$\frac{1}{4}\frac{\partial u}{\partial t} - v_0(1 + \epsilon e^{i\omega t})\frac{\partial u}{\partial y} = \epsilon\left(\frac{i\omega}{4} + Ha\right)e^{i\omega t} + \frac{\partial^2 u}{\partial y^2} + Gr(N\theta + \phi) - Ha(u - 1) \tag{3.3}$$

$$\frac{1}{4}\frac{\partial \theta}{\partial t} - v_0(1 + \epsilon e^{i\omega t})\frac{\partial \theta}{\partial y} = \left(\frac{1 + \alpha}{Pr}\right)\frac{\partial^2 \theta}{\partial y^2} + \beta\theta \tag{3.4}$$

$$\frac{1}{4}\frac{\partial \emptyset}{\partial t} - v_0(1 + \epsilon e^{i\omega t})\frac{\partial \phi}{\partial y} = \frac{1}{Sc}\frac{\partial^2 \phi}{\partial y^2} - \epsilon\lambda\phi\theta^n e^{\frac{\theta}{1+\epsilon\theta}} \tag{3.5}$$

and together with the boundary conditions (3.12) now being

$$\begin{rcases} t = 0: \quad u = 1, \quad \theta = 1, \quad \phi = 1, \quad \forall y \\ t > 0: \begin{cases} u = V, \theta = 1 + \epsilon e^{i\omega t}, \phi = 1 + \epsilon e^{i\omega t}, y = 0 \\ u = 1 + \epsilon e^{i\omega t}, \theta \to 0, \phi \to 0 \; as \; y \to \infty \end{cases} \end{rcases} \quad (3.6)$$

So also, the entropy generation Γ_n given as

$$\Gamma_n = \underbrace{\left(\frac{\partial \theta}{\partial y}\right)^2}_{\text{Thermal irreversibility}} + \underbrace{\delta_1 \left(\frac{\partial u}{\partial y}\right)^2}_{\text{Viscous irreversibility}} + \underbrace{\delta_2 \left(\frac{\partial \phi}{\partial y}\right) + \delta_3 \left(\frac{\partial \theta}{\partial y}\right)\left(\frac{\partial \phi}{\partial y}\right)}_{\text{Di□usive irreversibility}}$$

Where

$$\Gamma_{n,\theta} = \left(\frac{\partial \theta}{\partial y}\right)^2, \Gamma_{n,u} = \delta_1 \left(\frac{\partial u}{\partial y}\right)^2, \Gamma_{n,\phi} = \delta_2 \left(\frac{\partial \phi}{\partial y}\right), \Gamma_{n,D} = \delta_3 \left(\frac{\partial \theta}{\partial y}\right)\left(\frac{\partial \phi}{\partial y}\right)$$

Dimensionless terms denoted $\delta_i, (1 \leq i \leq 3)$, and called irreversibility distribution ratios, are given by:

$$\delta_1 = \frac{T_0 v_0}{K} \frac{\mu U_0^2}{T_0}, \delta_2 = \frac{T_0 C_0 R D v_0}{K}, \delta_3 = \frac{T_0 C_0 R D}{K}$$

The dimensionless total entropy generation is the integral *sum* over the system volume of the dimensionless local entropy generation

$$\Gamma_{n,T} = \int_\Omega \Gamma_n d\Omega$$

Thus

$$\Gamma_n = \left(\frac{\partial \theta}{\partial y}\right)^2 + \delta_1 \left(\frac{\partial u}{\partial y}\right)^2 + \delta_2 \left(\frac{\partial \phi}{\partial y}\right) + \delta_3 \left(\frac{\partial \theta}{\partial y}\right)\left(\frac{\partial \phi}{\partial y}\right) \quad (3.7)$$

It is quite essential to calculate the significant input of each source of entropy production in a system, in view of this, the Bejan number describes the proportion of the entropy production by heat transfer to the total proportion as represented in equation (37),

$$Be = \frac{\Gamma_{n,\theta}}{E_G} = \frac{\Gamma_{n,\theta}}{\Gamma_{n,\theta} + \Gamma_{n,u} + \Gamma_{n,d}} \quad (3.8)$$

It is important to note that the entropy generation due to diffusion ($\Gamma_{n,d} = \Gamma_{n,\phi} \, \Gamma_{n,\tau}$) is the sum of a pure term ($\Gamma_{n,\phi}$) which involves concentration gradient only and a crossed term ($\Gamma_{n,\tau}$) with both thermal and concentration gradients. Therefore, a coupling effect between thermal gradient and concentration gradient can be shown in the expression of the entropy generation, whereas this coupling effect was neglected in the energy and specie conservation equations (Soret and Dufour effects) and also in the mass diffusion flux equation (first Fick's law).

Bejan number ranges from 0 to 1. Accordingly, $Be \cong 1$ is the limit at which the heat transfer irreversibility dominates, $Be \cong 0$ is the opposite limit at which the irreversibility is dominated by fluid friction effects, and $Be = 1/2$ is the case in which the heat transfer and fluid friction entropy generation rates are equal.

IV. **Method of Solution**

To obtain the entropy generation, we first sought for the solution of non-dimensional equations (3.3) – (3.5) with the prescribed initial and boundary conditions (3.6), perturbation method in ϵ – neighborhood is used, as similar to the one used by [25], [26], [29], [30]; [31] and [32] was adopted in seeking for solution in this work. To this end, the velocity, temperature, and specie concentration fields are respectively defined by:

$$\begin{aligned} u(y,t) &= f_0(y) + \epsilon e^{i\omega t} f_1(y), \\ \theta(y,t) &= g_0(y) + \epsilon e^{i\omega t} g_1(y), \\ \phi(y,t) &= h_0(y) + \epsilon e^{i\omega t} h_1(y). \end{aligned} \quad (3.9)$$

The system of the governing equations reduces **to**

$$f_0'' + v_0 f_0' - Ha f_0 = -Gr(Ng_0 + h_0) - Ha = 9$$
$$g_0'' + \frac{Prv_0}{1+\alpha} g_0' + \frac{Pr\beta}{1+\alpha} g_0 = 0 \qquad (3.10a)$$
$$h_0'' + Scv_0 h_0' - \epsilon\lambda Sch_0 (g_0)^n e^{g_0} = 0$$
$$y = 0 : f_0 = V, g_0 = 1, h_0 = 1, \qquad (3.11a)$$
$$y \to \infty : f_0 \to 1, g_0 \to 0, h_0 \to 0,$$

and

$$g_1'' + \frac{Prv_0}{1+\alpha} g_1' + \frac{Pr}{1+\alpha}\left(\beta - \frac{i\omega}{4}\right) g_1 = -\frac{Prv_0}{1+\alpha} g_0'$$
$$h_1'' + Scv_0 h_1' - \frac{i\omega}{4} Sch_1 = -Scv_0 h_0' \qquad (3.10b)$$
$$f_1'' + v_0 f_1' - \left(Ha + \frac{i\omega}{4}\right) f_1 = -Gr(Ng_1 + h_1) - v_0 f_0' - \left(Ha + \frac{i\omega}{4}\right)$$
$$y = 0 : f_1 = 0, g_0 = 1, h_0 = 1, \qquad (3.11b)$$
$$y \to \infty : f_0 \to 1, g_0 \to 0, h_0 \to 0,$$

From the above, the mean solution of temperature, concentration and velocity respectively are,

$$g_0(y) = e^{-my}$$
$$h_0(y) = (1+\epsilon a_3) e^{-S_c v_0 y} + \epsilon \sum_{r=0}^{k} \frac{a_4}{r!} e^{-[m(n+r)+S_c v_0]y} \qquad (3.12)$$
$$f_0(y) = 1 + a_5 e^{-n_1 y} + a_6 e^{-my} + a_7 e^{-S_c v_0 y} + \sum_{r=0}^{k} a_8 \frac{a_4}{r!} e^{-[m(n+r)+S_c v_0]y}$$

Also, the oscillating solution of temperature, concentration and velocity respectively are,

$$g_1 = (1-a_2) e^{-m_1 y} + a_2 e^{-my}$$
$$h_1 = a_9 e^{-qy} + a_{10} e^{-Scv_0 y} + \sum_{r=0}^{k} \frac{a_{11}}{r!} e^{-[m(n+r)+Scv_0]y}$$
$$f_1 = 1 + a_{12} e^{-\tau y} + a_{13} e^{-m_1 y} + a_{14} e^{-my} + a_{15} e^{-qy} + a_{16} e^{-S_c v_0 y}$$
$$+ a_{17} e^{-n_1 y} + \sum_{r=0}^{k} \frac{a_{18}}{r!} e^{-(m(n+r)+Scv_0)y}$$

Where

$$m = \frac{Prv_0 + \sqrt{Pr^2 v_0^2 - 4Pr\beta(1+\alpha)}}{2(1+\alpha)}, m_1 = \frac{Prv_0 + \sqrt{Pr^2 v_0^2 - 4Pr(1+\alpha)(\beta - \frac{i\omega}{4})}}{2(1+\alpha)}, \tau = \frac{v_0 + \sqrt{v_0^2 + 4\left(Ha + \frac{i\cdot\omega}{4}\right)}}{2}, \beta \le \frac{Prv_0^2}{4(1+\alpha)}, a_2 = -\frac{mPrv_0}{(1+\alpha)m^2 - mPrv_0 + Pr\left(\beta - \frac{i\omega}{4}\right)}, a_3 = -\sum_{r=0}^{k} \frac{a_4}{r!}, a_4 = -\frac{\lambda Sc}{m(n+r)(m(n+r)+S_c v_0)}, a_6 = -\frac{GrN}{m^2 - mv_0 - Ha}, a_7 = -\frac{Gr\left(1 - \varepsilon \sum_{r=0}^{k} \frac{a_4}{r!}\right)}{S_c^2 v_0^2 - S_c v_0^2 - Ha}, n_1 = \frac{v_0 + \sqrt{v_0^2 + 4Ha}}{2}$$

$$a_8 = -\frac{\varepsilon Gr}{(m(n+r)+S_c v_0)^2 - v_0(m(n+r)+S_c v_0) - Ha}, a_{10} = -\frac{4Scv_0^2(1+\epsilon a_3)}{i\omega}, a_{11} = \frac{\epsilon a_4 Scv_0(m(n+r)+Scv_0)}{m(n+r)(m(n+r)+Scv_0) - \frac{i\omega}{4} Sc}, a_{13} = -\frac{GrNa_1}{m_1^2 - v_0 m_1 - \left(Ha + \frac{i\omega}{4}\right)}$$

$$a_{14} = \frac{v_0 a_6 m - GrNa_2}{m^2 - v_0 m - \left(Ha + \frac{i\omega}{4}\right)}, a_{15} = -\frac{Gra_9}{q^2 - v_0 q - \left(Ha + \frac{i\omega}{4}\right)}$$

$$a_{16} = \frac{a_7 Scv_0^2 - Gra_{10}}{Sc^2 v_0^2 - Scv_0^2 - \left(Ha + \frac{i\omega}{4}\right)}, a_{17} = \frac{v_0 a_5 n_1}{n_1^2 - v_0 n_1 - \left(Ha + \frac{i\omega}{4}\right)}$$

$$a_{18}=\frac{v_0a_8a_4(m(n+r)+Scv_0)-Gra_{11}}{(m(n+r)+Scv_0)(m(n+r)+Scv_0-v_0)-\left(Ha+\frac{i\omega}{4}\right)}$$

$$a_{12}=-\left(1+a_{13}+a_{14}+a_{15}+a_{16}+a_{17}+\sum_{r=0}^{k}\frac{a_{18}}{r!}\right)$$

The expression for the velocity temperature and Concentration thus becomes

$$\begin{aligned}u(y,t)&=1+a_5e^{-n_1y}+a_6e^{-my}+a_7e^{-S_cv_0y}+\sum_{r=0}^{k}a_8\frac{a_4}{r!}e^{-[m(n+r)+S_cv_0]y}\\&+\epsilon e^{i\omega t}\{1+a_{12}e^{-\tau y}+a_{13}e^{-m_1y}+a_{14}e^{-my}+a_{15}e^{-qy}+a_{16}e^{-S_cv_0y}\\&+a_{17}e^{-n_1y}+\sum_{r=0}^{k}\frac{a_{18}}{r!}e^{-(m(n+r)+Scv_0)y}\Big\}\end{aligned}\tag{3.13}$$

$$\theta(y,t)=\ e^{-my}+\ \epsilon e^{i\omega t}\{a_1e^{-m_1y}+a_2e^{-my}\}\tag{3.14}$$

$$\begin{aligned}\phi(y,t)=&\ (1+\epsilon a_3)e^{-Scv_0y}+\epsilon\sum_{r=0}^{k}\frac{a_4}{r!}e^{-[m(n+r)+Scv_0]y}\\&+\epsilon e^{i\omega t}\left\{a_9e^{-qy}+a_{10}e^{-Scv_0y}+\sum_{r=0}^{k}\frac{a_{11}}{r!}e^{-[m(n+r)+Scv_0]y}\right\}\end{aligned}\tag{3.15}$$

Therefore, Entropy generation and Bejan number equations are obtained by substituting (3.13) - (3.15) into (3.7) and (3.8) respectively and apply Maple in-built evalc package to decompose both entropy and Bejan number equations into real and imaginary parts. After some algebra, the real parts are:

$$\begin{aligned}\Gamma_n=&\ m^2(\exp(-my))^2+\delta_1\begin{pmatrix}-a_5n_1\exp(-n_1y)-a_6m\exp(-my)-a_7Scv_0\exp(-Scv_0y)\\+K[1](-m(n+r)-Scv_0)\exp(-(m(n+r)+Scv_0)y)\end{pmatrix}^2\\&+\delta_2\begin{pmatrix}-(a_3\varepsilon+1)Scv_0\exp(-Scv_0y)\\-\varepsilon K[2](-m(n+r)-Scv_0)\exp(-(m(n+r)+Scv_0)y)\end{pmatrix}^2\\&-\delta_3m\exp(-my)\,(-(a_3\varepsilon+1)Scv_0\exp(-Scv_0y)\\&-\varepsilon K[2](-m(n+r)-Scv_0)\exp(-(m(n+r)+Scv_0)y)\end{aligned}\tag{3.16}$$

$$Be:=\frac{m^2(\exp(-my))^2}{\left(\begin{aligned}&m^2(\exp(-my))^2+\delta_1\begin{pmatrix}-a_5n_1\exp(-n_1y)-a_6m\exp(-my)-a_7Scv_0\exp(-Scv_0y)\\+K[1](-m(n+r)-Scv_0)\exp(-(m(n+r)+Scv_0)y)\end{pmatrix}^2\\&+\delta_2\begin{pmatrix}-(a_3\varepsilon+1)Scv_0\exp(-Scv_0y)\\-\varepsilon K[2](-m(n+r)-Scv_0)\exp(-(m(n+r)+Scv_0)y)\end{pmatrix}^2\\&-\delta_3m\exp(-my)\,(-(a_3\varepsilon+1)Scv_0\exp(-Scv_0y)\\&-\varepsilon K[2](-m(n+r)-Scv_0)\exp(-(m(n+r)+Scv_0)y)\end{aligned}\right)}\tag{3.17}$$

V. Results and discussion

A code was written to display contours plot with labels executed by computational software Maple 2022 version. The resulting graphs and discussion are given below.

Entropy generation in unsteady oscillatory magnetohydrodynamic (MHD) flow with thermal radiation and binary chemical reaction is crucial for characterizing irreversibilities and energy dissipation. It serves as a fundamental metric for assessing process efficiency and performance. Analyzing entropy generation helps identify areas of high inefficiency, guiding optimization efforts to minimize energy losses and improve system performance.

In this context, entropy generation offers insights into the interplay between fluid dynamics, heat transfer, and chemical reactions, aiding in process efficiency improvement, resource conservation, and environmental impact mitigation. It also facilitates the design and optimization of advanced technologies across engineering fields. Our attention is directed toward analyzing the result by considering:

1. Regions of High and Low Scalar Values on a Contour Graph:
   (i) Contour Lines:

- Densely packed contour lines signify rapid change or steep gradients in the scalar field, indicating higher or lower scalar values respectively.
- High variability in the scalar field is indicated by densely packed contour lines.

(ii) Scalar Value Labels:

- Numeric labels on contour lines with higher values correspond to regions of higher scalar values, while lower values represent regions of lower scalar values.
- Clustered contour lines with higher numeric labels suggest regions with higher scalar values.

2. Critical Points such as Maxima and Minima:

(i) Peak or Valley Patterns:

- Peaks resemble local maxima, surrounded by contour lines with decreasing scalar values, while valleys represent local minima, surrounded by contour lines with increasing scalar values.

(ii) Isolated Points:

- Points where contour lines come together or form closed loops indicate critical points such as maxima, minima, or saddle points.

3. Spatial Patterns or Trends in the Data:

(i) Overall Trend: Observe the general trend of contour lines across the graph, whether they are uniformly spaced or irregularly distributed, and identify areas with denser or sparser contour lines.

(ii) Gradient Direction: Pay attention to the direction in which contour lines bend or curve; sharp bends indicate rapid changes in the scalar field, while gentle curves suggest more gradual changes.

Notably, temperature emerges as the most influential factor in entropy generation, indicated by its highest numerical values, followed by chemical species concentration, while velocity shows the lowest impact. Effect of Hartmann number on entropy and Grashof number were displayed in Figure 1 and 3 respectively. An increased Hartmann number reduces fluid velocity due to the stronger Lorentz force, leading to enhanced viscous dissipation and Joule heating. This alters heat transfer characteristics, which can be either enhanced or reduced depending on specific conditions. Overall, it results in increased entropy generation due to the combined effects of higher thermal and frictional entropy generation from greater viscous dissipation and Joule heating while, an increased Grashof number typically leads to enhanced buoyancy-driven flow and heat transfer, resulting in higher thermal entropy generation. The overall entropy generation in the system increases due to the combined effects of thermal and frictional entropy mechanisms. The buoyancy ratio (N), depicted in Figure 5, plays a pivotal role in buoyancy-driven flows like natural convection, where increasing N intensifies buoyancy forces over viscous forces, notably impacting entropy generation, especially away from surfaces. Higher oscillation frequencies (ω), as shown in Figure 7, introduce rapid flow changes, leading to enhanced entropy generation due to increased viscous dissipation and flow unsteadiness.

Heat generation/absorption (β), illustrated in Figure 9, significantly influences entropy generation by introducing additional energy sources or sinks within fluid flow systems. Meanwhile, generative or destructive chemical reactions (λ), depicted in Figure 11, can either release or absorb energy, consequently impacting entropy generation. Additionally, the pre-exponential parameter (α), as shown in Figure 13, highlights the significance of chemical reaction rates in influencing entropy generation.

The systems consider in this work is one in which heat and mass transfer processes are coupled, the irreversibilities from both mechanisms interact, describing the relative contributions of viscous, thermal and mass diffusive entropy generation. These coupled diffusion processes enhance overall entropy generation rates due to their nonlinear interaction. This phenomenon are displayed in Figures 15, 17 and 19 respectively, the combined diffusion processes significantly increase entropy generation. Viscous irreversibility increases entropy generation through enhanced viscous dissipation, affected by fluid viscosity and velocity gradients, especially significant in high-velocity or high-viscosity flows. Mass diffusion irreversibility generates entropy due to concentration gradients, influenced by the magnitude of these gradients and the diffusivity of species, crucial in multicomponent systems with substantial mass transfer. The combined effect of coupled thermal and mass diffusive irreversibility results in higher overall entropy generation due to the synergistic effects of interacting temperature and concentration gradients, making it essential to understand these contributions for optimizing systems to minimize irreversibility and improve efficiency.

The Bejan number, a dimensionless parameter illustrated in Figures 2, 4, 6, …20, offers valuable insights into system efficiency by quantifying irreversibilities associated with heat transfer processes. Its analysis aids in discerning dominant entropy generation mechanisms and guiding optimizations to enhance system performance.

By comparing the Bejan number to unity, engineers can prioritize modifications for improved efficiency in heat transfer processes and fluid flow systems, facilitating the development of more efficient and sustainable solutions. Additionally, the Bejan number serves as a crucial design guideline, aiding in interpreting research findings and identifying areas for further investigation, ultimately enabling the development of more efficient solutions in various engineering applications.

From Figures $2, 4, 6, \ldots, 20$, a critical analysis of indicates the followings:

1. **High Variability:** A wide range of values suggests that the variable under consideration exhibits substantial variation across the spatial domain represented in the contour graph. This variability indicates heterogeneous conditions, complex interactions, as well as interplay and interaction between the flow conditions phenomena within the system under study.

2. **Complexity:** A large range of values often reflects the complexity of the underlying physical processes or phenomena. It signifies the presence of multiple contributing factors, nonlinear relationships, or intricate spatial patterns that influence the distribution of the variable being depicted in the contour graph.

3. **Sensitivity to Parameters:** The wide range of values indicate that the variable of interest is highly sensitive to changes in input parameters or boundary conditions. Small alterations in system parameters can lead to significant variations in the variable's distribution, highlighting the importance of parameter sensitivity analysis and robust modeling techniques.

4. **Critical Zones:** Within the contour graph, regions associated with extreme values or sharp transitions between contour lines represent critical zones or areas of particular interest. These zones signify locations of maximum or minimum values, points of convergence or divergence, or regions where specific phenomena are concentrated.

Generally, a large range of values in a contour graph suggests complexity, variability, and sensitivity within the dataset, emphasizing the need for thorough analysis and interpretation to extract meaningful insights about the underlying physical processes or phenomena.

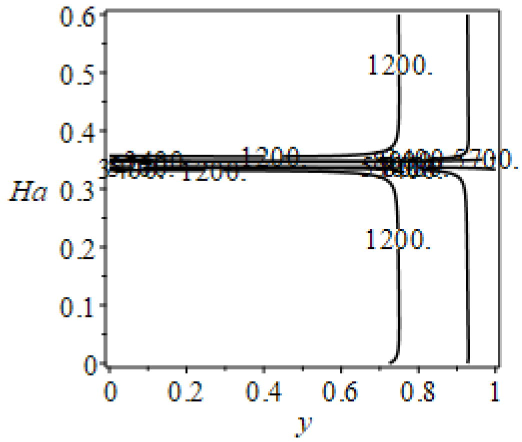

Figure 1: Effect of Hartmann number on Entropy generation

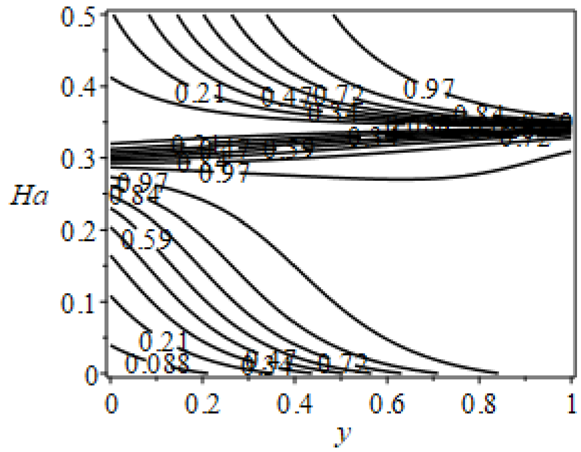

Figure 2: Effect of Hartmann number on Bejan number

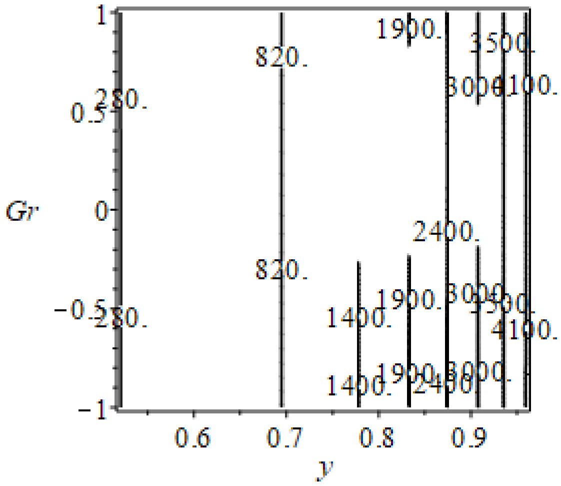

Figure 3: Influence of Grashof term on Entropy Generation

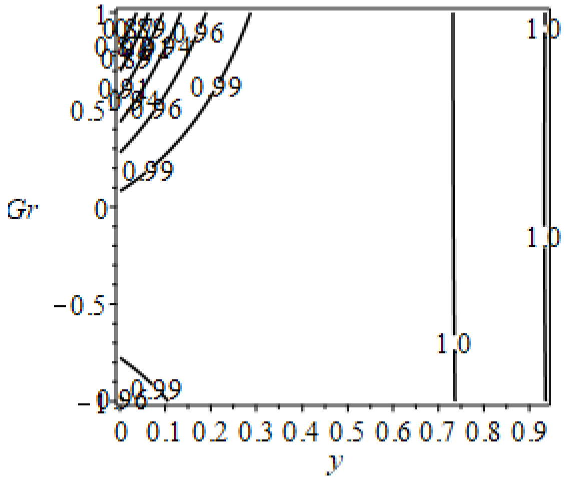

Figure 4: Influence of Grashof term of Bejan number

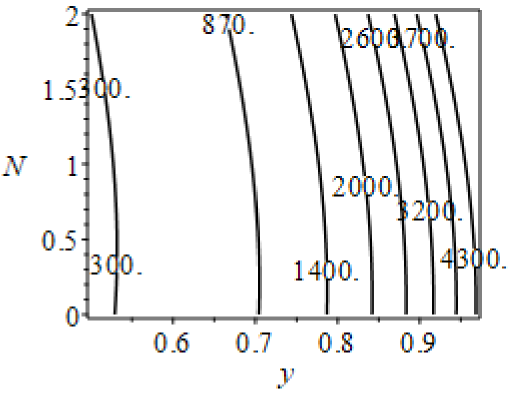

Figure 5: Effect of Buoyancy ratio on entropy generation

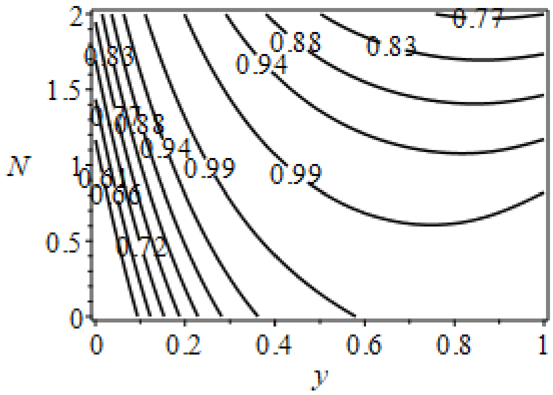

Figure 6: Effect of Buoyancy ratio on Bejan number

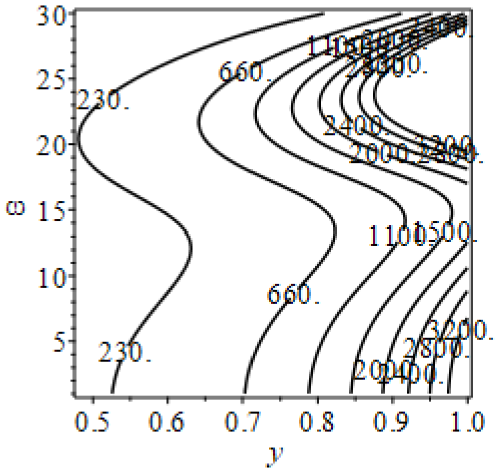

Figure 7: Effect of oscillation factor on entropy generation

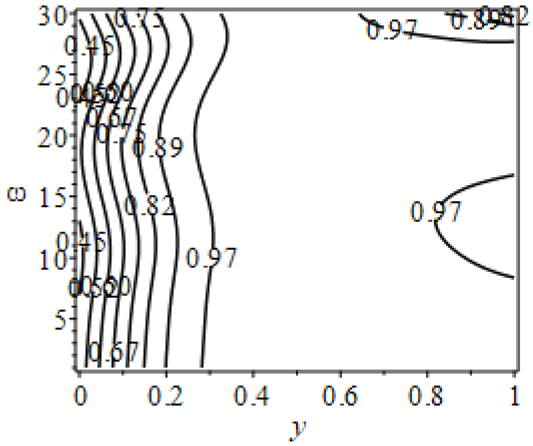

Figure 8: Effect of oscillation factor on Bejan number

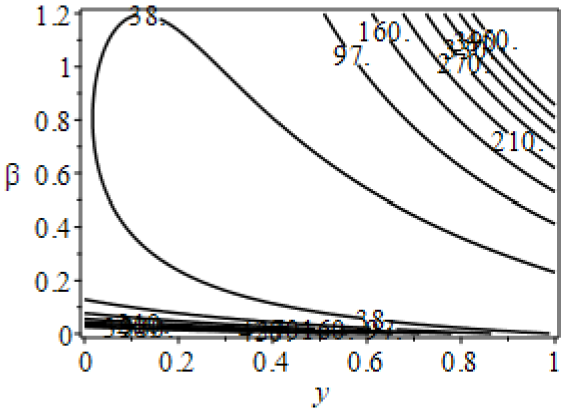

Figure 9: Effect of heat generation on entropy generation

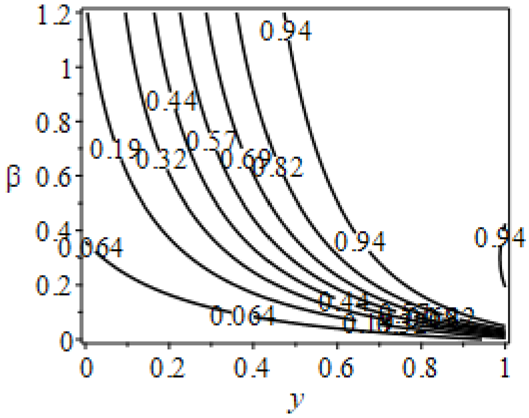

Figure 10: Effect of heat generation on Bejan number

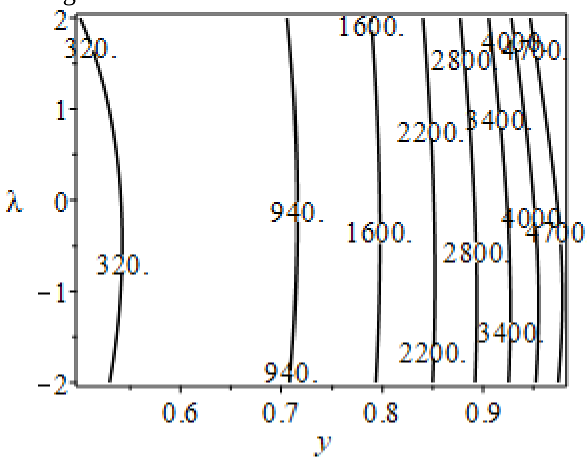

Figure 11: Impact of chemical reactivity on entropy generation

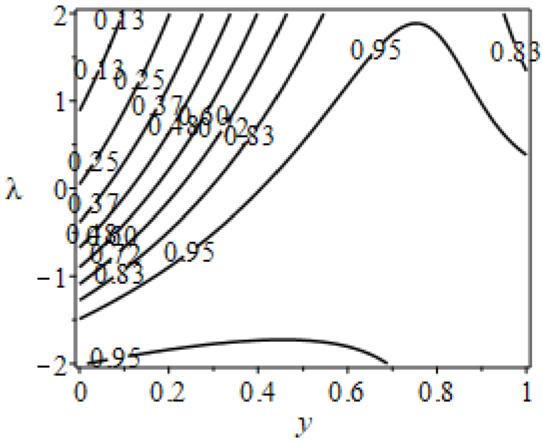

Figure 12: Impact of chemical reactivity on Bejan number

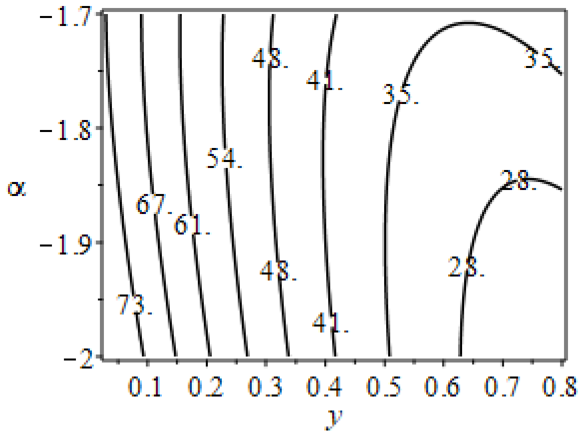

Figure 13: Influence of pre-exponential factor on entropy generation

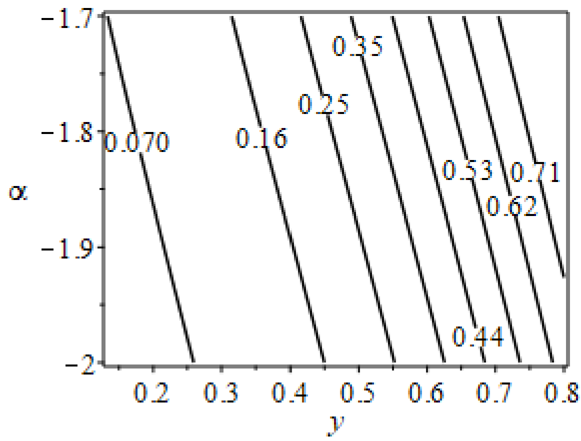

Figure 14: Influence of pre-exponential factor on Bejan number

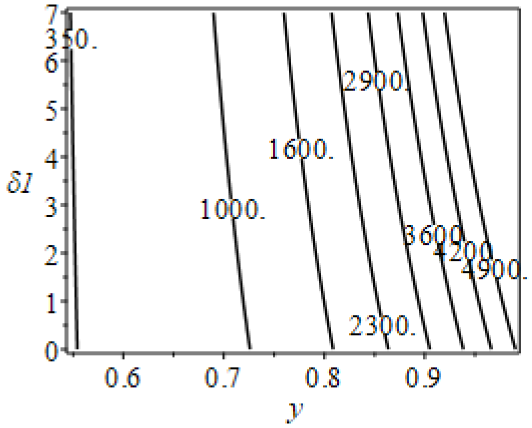

Figure 15: Impact of viscous irreversibility on entropy generation

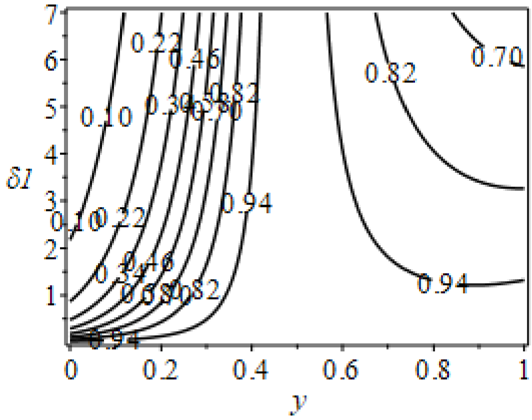

Figure 16: Impact of viscous irreversibility on Bejan number

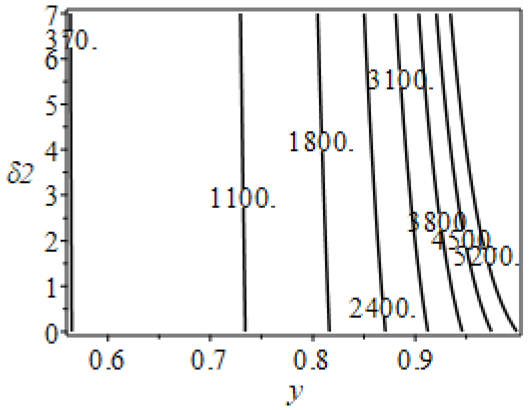

Figure 17: Impact of Mass Diffusive irreversibility on entropy generation

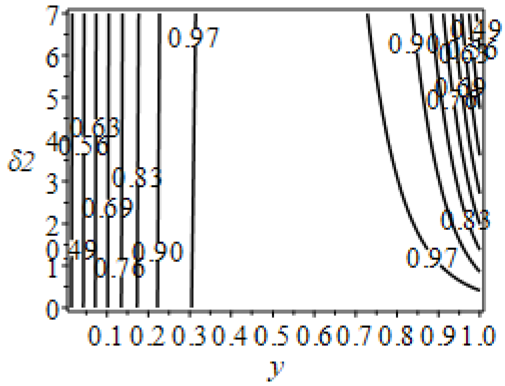

Figure 18: Impact of Mass Diffusive irreversibility Bejan number

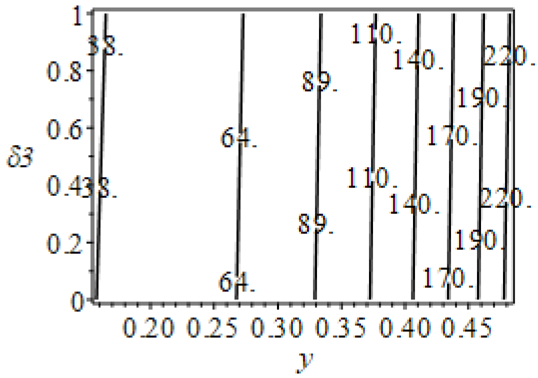

Figure 19: Effect of coupled themal and mass Diffusive irreversibility on entropy generation

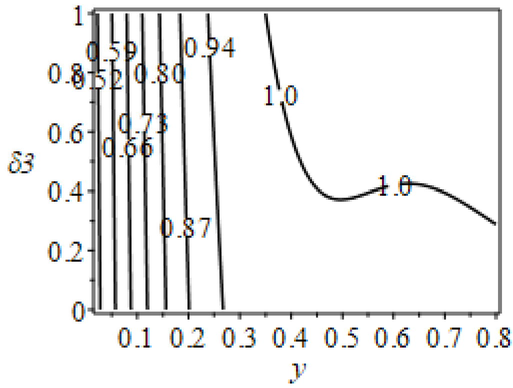

Figure 20: Effect of coupled themal and mass Diffusive irreversibility on Bejan number

5.1 Summary of Research work

This research investigates unsteady oscillatory magnetohydrodynamic (MHD) flow past a moving plate, considering thermal radiation and binary chemical reactions. It aims to unravel entropy generation complexities, crucial for understanding irreversibilities. By exploring fluid dynamics, electromagnetism, heat transfer, and chemical kinetics interplay, it offers profound insights beyond disciplinary boundaries. At its core lies second law analysis, crucial in unsteady MHD flow where electrically conducting fluids interact with magnetic fields, compounded by oscillatory flow dynamics. Thermal radiation's inclusion adds complexity, influencing energy distribution and temperature profiles. Binary chemical reactions further alter flow dynamics, elucidating their contribution to entropy generation. This interdisciplinary approach integrates principles from various fields, employing advanced mathematical modeling techniques to simulate complex flow scenarios. Through rigorous analysis, it quantifies entropy generation, offering insights for system optimization. Beyond theoretical understanding, findings inform practical system design in aerospace, renewable energy, chemical processing, and environmental engineering, contributing to knowledge advancement and technological innovation.

5.2 Observation and Conclusion

The study investigates the second law analysis of unsteady oscillatory Magnetohydrodynamic (MHD) flow past a moving plate with thermal radiation and binary chemical reaction, yielding valuable insights into the thermodynamic behavior of complex fluid systems. By integrating principles from fluid mechanics, electromagnetism, heat transfer, and chemical engineering, the research advances understanding of entropy generation mechanisms and their impact on system efficiency. The observations underscore the intricate interplay between various physical phenomena, including flow unsteadiness, magnetic fields, thermal radiation, and chemical reactions, necessitating a comprehensive analysis approach. The findings have significant implications for engineering practice, guiding the design and optimization of systems in aerospace engineering, renewable energy, chemical processing, and environmental engineering. Through quantifying entropy generation rates and assessing thermodynamic efficiency metrics, the study offers valuable tools for enhancing the performance and sustainability of engineering systems.

As a result of the analysis and discussion of results of this research, the following are deduced:

1. Dynamic fluctuations in velocity, temperature, and magnetic field strength highlight the complexity of the system dynamics, necessitating thorough analysis.
2. Higher oscillation frequencies exacerbate irreversibilities, emphasizing the need for strategies to mitigate entropy-related losses.
3. Alterations in flow dynamics due to Lorentz forces demonstrate the significant role of magnetic fields in shaping system behavior and entropy generation rates.
4. The significant contribution of thermal radiation to entropy generation emphasizes its importance in heat transfer processes and system efficiency.
5. Introduction of complexities due to chemical reactions highlights their influence on system behavior and entropy generation.
6. Faster reaction rates leading to higher irreversibilities emphasize the importance of accounting for chemical kinetics in optimizing system performance and minimizing losses.

REFERENCES

[1]. Soundalgekar, V. (1979), ‘Free convective eff ects on the flow past a vertical oscillating plate’, *Astrophysics and Space Science* **64**, 165–172.

[2]. Bergstrom, R. (1976), ‘Viscous boundary layers in rotating fluids driven by periodic flows’, *journal of Atmospheric Sciences (J Atmos Sci* **33**, 1234–1247.

[3]. Nazar R., Amin N. I. P. (2004), ‘Unsteady boundary layer flow due to a stretching surface in a rotating fluid’, *Mechanics Research Communications (Mech Res Commun* **31**, 121–128.

[4]. Zheng L. and Li C. and Zhang X. and Gao. Y. (2011), ‘Exact solutions for the unsteady rotating flows of a generalized maxwell fluid with oscillating pressure gradient between coaxial cylinders’, *Computers and Mathematics with Applications* **62**, 1105–1115.

[5]. Chamkha, A.J., Rashad, A.M., and Al-Mudhaf, H. (2012). Heat and mass transfer from a truncated cone with variable wall temperature and concentration in the presence of chemical reaction effects. *International Journal of Numerical Methods for Heat and Fluid Flow*, 22, 357–376.

[6]. H. Waqas and S.U. Khan and, M. Imranand M.M. Bhatti. (2019), ‘Thermally developed falkner–skan bioconvection flow of a magnetized nanofluid in the presence of motile gyrotactic microorganism: Buongiorno’s nanofluid model’, *Physica Scripta* **94**(11), 432–443.

[7]. Nguyen-Thoi T. and Bhatti M.M. and Ali J.A. and Hamad S.M. and Sheikholeslami M. and Shafee A. and R-Haq U. (2019), ‘Analysis on the heat storage unit through a y-shaped fn for solidifcation of nepcm’, *journal of Molecular Liquids* **292**, 111378.

[8]. Maleque, K. (2013), ‘Unsteady natural convection boundary layer flow with mass transfer and a binary chemical reaction’, *British journal of Applied Science and Technology* **3**, 131–149.

[9]. Mallikarjuna, B. & A.M. Rashad, A.J. Chamkha, S. R. (2015), ‘Chemical reaction eff ects on MHD convective heat and mass transfer flow past a rotating vertical cone embedded in a variable porosity regime’, *Afrika Matematika* **27**, 645–653.

[10]. Zhang C. and Zhengand L., Zhang X. and Chen. G. (2015), ‘Mhd flow and radiation heat transfer of nanofluid in porous media with variable surface heat flux and chemical reaction’, *Applied Mathematics and Modelling* **39**, 165–172.

[11]. Abbas Z. , Sheikh M., Motsa S.S., Numerical solution of binary chemical reaction on stagnation point flow of Casson fluid over a stretching/shrinking sheet with thermal radiation, Energy, Volume 95, 2016, Pages 12-20, ISSN 0360-5442, https://doi.org/10.1016/j.energy.2015.11.039.
[12]. Shercliff, J. A. (1965). A Textbook of Magnetohydrodynamics. Pergamon Press.
[13]. [13] Moreau, R. (1990). Magnetohydrodynamics. Springer.
[14]. Pop, I., & Ingham, D. B. (2001). Convective Heat Transfer: Mathematical and Computational Modelling of Viscous Fluids and Porous Media. Pergamon.
[15]. Modest, M. F. (2013). Radiative Heat Transfer. Academic Press.
[16]. Bird, R. B., Stewart, W. E., & Lightfoot, E. N. (2002). Transport Phenomena. John Wiley & Sons.
[17]. Kishore, P. V. R., & Bhattacharyya, K. (2014). Entropy generation due to MHD flow in a vertical channel with temperature dependent source/sink. International Journal of Heat and Mass Transfer, 70, 380-390.
[18]. Bejan, A. (1996). Entropy Generation Minimization: The Method of Thermodynamic Optimization of Finite-Size Systems and Finite-Time Processes. CRC Press.
[19]. Bejan, A., & Dincer, I. (2002). Thermodynamic Optimization of Complex Energy Systems. Springer.
[20]. Aung, W., & Worku, G. (1986). Theory of fully developed, combined convection including flow reversal. Journal of Heat Transfer, 108(2), 485-488.
[21]. Gebhart, B., Jaluria, Y., Mahajan, R. L., & Sammakia, B. (1988). Buoyancy-Induced Flows and Transport. Hemisphere Publishing Corporation.
[22]. Hassanien, I. A., Al-Sanea, S. A., & Al-Amiri, A. M. (1998). The effect of variable properties on laminar free convective heat and mass transfer in a vertical channel. International Journal of Heat and Mass Transfer, 41(17), 2731-2742.
[23]. Abo-Dahab S.M., Mahmoud Ragab, Azhari A. Elhag, Abdel-Khalek S. Free convection effect on oscillatory flow using artificial neural networks and statistical techniques. Alexandria Engineering Journal, Volume 59, Issue 5, 2020, Pages 3599-3608, https://doi.org/10.1016/j.aej.2020.06.005.
[24]. Abdelhameed, T.N. Entropy generation of MHD flow of sodium alginate ($C_6H_9NAO_7$) fluid in thermal engineering. Sci Rep **12**, 701 (2022). https://doi.org/10.1038/s41598-021-04655-0
[25]. Okedoye, A. & Ogunniyi, P. (2019), 'Mhd boundary layer flow past a moving plate with mass transfer and binary chemical reaction', *Journal of Nigeria Mathematical Society* **38**(1), 89–121.
[26]. Okedoye, A. & Salawu, S. (2019*b*), 'Unsteady oscillatory mhd boundary layer flow past a moving plate with mass transfer and binary chemical reaction', *SN Applied Sciences* **1**(1586).
[27]. Okedoye, A. M., Salawu, S. O. & Asibor, R. E. (2021), 'A convective mhd double diffusive flow of a binary mixture through an isothermal and porous moving plate with activation energy', *Computational Thermal Sciences* **13**(5
[28]. Magherbi, M. and Abbassi, H. and Hidouri, N. and Ben Brahim, A. (2006), 'Second law analysis in convective heat and mass transfer,', *Entropy*, **8**, 1–17
[29]. Lighthill, M. (1954), 'The response of laminar skin friction and heat transfer to fluctuations in the stream velocity', *Proceedings of the Royal Society of London. Series A, Mathematical and Physical Sciences* **224**, 1–23.
[30]. Okedoye, A. & Salawu, S. (2019*a*), 'Eff ect of nonlinear radiative heat and mass transfer on mhd flow over a stretching surface with variable conductivity and viscosity', *Journal of the Serbian Society for Computational Mechanics* **13**(2), 87–104.
[31]. 31. Okedoye, A. & Salawu, S. (2020), 'Transient heat and mass transfer of hydromagnetic eff ects on the flow past a porous medium with movable vertical permeable sheet', *International Journal of Applied Mechanics and Engineering* **25**(4)
[32]. 32. Akpabokigho, L. P., Akinyemi, O. A. & Okedoye, A. M. (2023), 'Entropy generation in unsteady mhd convective flow past a flat porous oscillating plate with suction or injection', *Global Journal of Engineering and Technology Advances* **14**(02), 107–127.